21
Whirls and vortices

Whirls and vortices are common features of real fluids. Stirring the coffee, you create a circulating motion, a whirl that dies out after some time when you stop stirring. A fast spinning vortex may be created at the drain of a bathtub when it is emptied, and it may remain quasi-stable as long as there is enough water in the tub. Normally, whirls and vortices are invisible far away from free boundaries, but in the bathtub the drain vortex is made visible by soap remains clouding the water and the depression it creates at the surface. It may even become audible, because water falling through the drain sucks air down from the surface.

In the atmosphere above heated ground, whirls and vortices arise all the time. Mostly they are small and invisible, but sometimes they pick up dust and debris and appear as dust devils. Larger dust devils, in some countries called sky-pumps, are known to pick up haystacks and scatter them, or to throw tables around in sidewalk cafes. When the heat-driven air vortices grow really big and nasty, they may become tornadoes. The force powering heat-driven vortices is the same as the force that maintains a bathtub vortex, namely gravity. In the bathtub the vortex is sustained by the gravity's work on the water falling through the drain, and in the atmosphere by its work on updrafts caused by the buoyancy of bubbles of hot air.

Vortices are also created in the wakes of moving objects. From the tips of the wings of aircraft there will always be invisible trailing vortices (to be discussed in chapter 26). Large passenger aircraft taking off or landing create strong and fairly stable vortices, capable of overturning smaller planes following after. "Beware of vortex" is a common warning issued by flight controllers to small aircraft during takeoff and approach to landing.

The focus of the chapter is on explicit models for non-singular vortices, and on the strong theorems due to Stokes, Kelvin and Helmholtz that give us insight into vortex dynamics in nearly ideal fluids. Extensive treatment of vortex structure and dynamics may be found in [43, 44].

21.1 The Rankine vortex

William John Macquorne Rankine (1820–72), Scottish engineer and physicist.

The spindle-driven vortex discussed on page 324 was powered by a rotating cylindrical spindle, which delivered the work necessary to overcome viscous friction in the fluid. Although the flow pattern (18-67) did not depend explicitly on the viscosity of the fluid, a finite viscosity was nevertheless necessary for the spindle to be able to "crank up" the vortex, starting from fluid at rest. In a truly inviscid (ideal) fluid we would not be able to crank up a vortex, but once it had somehow been established there would be no viscous losses and the vortex would keep spinning forever. The solid spindle could then with impunity be replaced by a *core* made from the same fluid as the vortex and rotating as a solid body with the same angular velocity as the spindle.

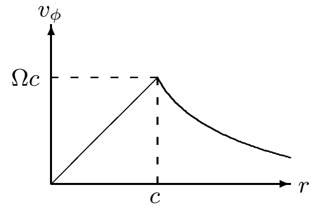

Sketch of the velocity field for the Rankine vortex. In a viscous fluid the cusp at the core boundary $r = c$ indicates a discontinuity in shear stress which is physically unacceptable.

A *Rankine vortex* with core radius c is constructed in precisely this way,

$$v_\phi = \begin{cases} \Omega\, r & 0 \le r \le c \\ \dfrac{\Omega c^2}{r} & c \le r < \infty \end{cases} . \tag{21-1}$$

Its vorticity vanishes outside the core and is constant inside(problem 18.27).

The effective pressure must supply the necessary centripetal force for the circulating motion, as expressed by (18-53a). Integrating that equation we obtain,

$$\frac{p^*(r)}{\rho_0} = \begin{cases} -(c^2 - \frac{1}{2}r^2)\Omega^2 & 0 \le r \le c\ , \\ -\dfrac{\Omega^2 c^4}{2r^2} & c \le r < \infty\ , \end{cases} \tag{21-2}$$

where the pressure inside the core has been joined continuously to the pressure outside. In constant gravity, the shape of an open liquid surface follows the effective pressure,

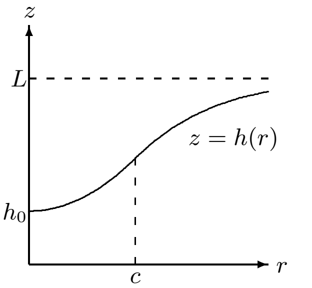

Sketch of the open surface shape $z = h(r)$ in a Rankine vortex.

$$z = h(r) = L + \frac{p^*}{\rho_0 g_0}\ , \tag{21-3}$$

where L is the asymptotic height of the liquid. The surface of the Rankine vortex continues all the way to $r = 0$ with a central depression,

$$L - h_0 = \frac{\Omega^2 c^2}{g_0}\ , \tag{21-4}$$

where $h_0 = h(0)$. The central depression is precisely the double of the depression, $L - h(c)$, at the core boundary.

Although the Rankine velocity field is continuous everywhere, it has a cusp at the core boundary. If the viscosity does not vanish, this cusp will produce a jump in shear stress (18-58) from $\sigma_{\phi r} = 0$ everywhere inside the core to $\sigma_{\phi r} = -2\eta\Omega$ just outside. Such a jump is physically unacceptable because it violates Newton's third law which requires continuity of the stress vector across any boundary. The Rankine vortex is only meaningful for a truly inviscid fluid.

21.2 Basic vortex dynamics

Vortex lines were defined (page 249) to be curves that everywhere follow the instantaneous vorticity field, $\boldsymbol{\omega} = \boldsymbol{\nabla} \times \boldsymbol{v}$. Like streamlines, vortex lines cannot cross each other, and since the vorticity field is divergence-free, $\boldsymbol{\nabla} \cdot \boldsymbol{\omega} = 0$, vortex lines cannot emerge from anywhere, but must form closed curves, or curves coming from and going to the boundaries of the flow (or to spatial infinity). Vortex dynamics is quite complicated [43, 44], and we shall here only present a few results that are mainly due to Helmholtz.

Hermann von Helmholtz (1821–94), Austrian polyhistor.

Vortex tubes

The set of vortex lines going through the points of a closed curve C at a given time t form together a *vortex tube* that may curve and bend in space. Whatever shape it takes, it will nevertheless have the same total flux of vorticity through every cross section, and by Stokes theorem (15-40) this flux equals the circulation around the tube. To prove this we just use Gauss' theorem on a stretch of vortex tube between two cross sections, S_1 and S_2. The sides of the tube cannot contribute, because the surface elements are orthogonal to the vortex lines, which leaves only the two contributions from the ends. Since $\boldsymbol{\nabla}\cdot\boldsymbol{\omega} = 0$ the closed surface integral over the stretch of tube must vanish,

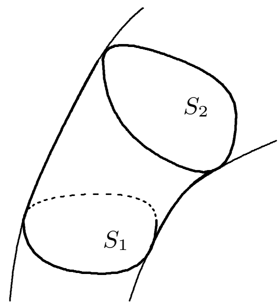

The flux of vorticity is the same in every cross section of a vortex tube.

$$\oint_S \boldsymbol{\omega} \cdot d\boldsymbol{S} = \int_{S_2} \boldsymbol{\omega} \cdot d\boldsymbol{S} - \int_{S_1} \boldsymbol{\omega} \cdot d\boldsymbol{S} = 0 \ . \tag{21-5}$$

The common flux through any cross section of a vortex tube is called the *strength* of the tube. For most vortices there will be a central vortex tube, called the *core* of the vortex, containing almost all of the vorticity.

Kelvin's circulation theorem (15-42) tells us furthermore that in an inviscid fluid a comoving vortex tube never changes its strength, independently of how it is blown around by the ambient flow. In this sense, a vortex acquires an identity of its own. It may connect to the boundaries (possibly at infinity), but often it will form a closed loop like a smoke ring moving around in space.

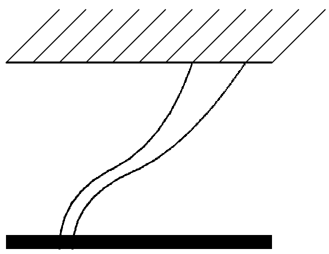

A tornado funnel may be viewed as a vortex filament connecting the ground and the thundercloud. Typically, the cloud moves and drags the top of the tornado along.

Vortex filaments

In the extreme and singular limit, where the vortex core becomes infinitely thin and its vorticity field infinitely high, it is called a *vortex filament*. The generic vortex filament is obtained from the Rankine vortex (21-1) by letting its radius vanish, $c \to 0$, and the angular velocity become infinite, $\Omega \to \infty$, so that $C = \Omega c^2$ remains constant. The field of the ideal filament then becomes

$$v_\phi = \frac{C}{r} \ , \tag{21-6}$$

with constant circulation $\Gamma = 2\pi C$. The vortex filament is here an infinitely thin straight line of vorticity connected to spatial infinity, but as discussed above it may move around, bend and twist without ever losing a turn, assuming that there is no viscosity. In reality viscosity will make the vortex cores expand, but if the time and distance scales are right real vortices will behave as filaments.

In section 15.7 we discussed vorticity-free flow and concluded that the velocity field may conveniently be represented as the gradient of a *velocity potential*, $\boldsymbol{v} = \boldsymbol{\nabla}\psi$. For the elementary vortex filament above, the velocity potential becomes

$$\psi = C\phi = C \arctan \frac{y}{x} \ , \tag{21-7}$$

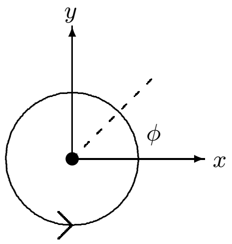

The multivalued angular dependence of the velocity potential of an elementary vortex filament reflects the vorticity carried in its core.

in either cylindrical or Cartesian coordinates. This may be verified by means of the cylindrical gradient operator (2-56). The Cartesian form is most convenient if one wishes to place the origin of the vortex somewhere else in the xy-plane.

In spite of the velocity being a single-valued function of space, the azimuthal angle ϕ is a multivalued function which increases by 2π each time one makes a complete circle around the origin. Alternatively, one may view the angle as being discontinuous with a jump of 2π somewhere, say at the x-axis. This peculiar behavior just reflects that space around the vortex is not simply connected. The singular center of the filament carries an infinite vorticity field so that the otherwise irrotational vortex gets a finite and constant circulation everywhere.

Interactions between line vortices

Vortices are not always loners like the bathtub vortex or the tornado, but may interact with other vortices or even with different parts of themselves, giving rise to a number of interesting phenomena. In ideal fluid, the only possible interaction is the advection of one vortex in the flow created by the others. Each vortex is in accordance with Kelvin's theorem blown around in the winds created by all the other vortices.

A pair of parallel vortex filaments with the same strength C and a distance d between the cores, will move in a circle of radius $d/2$ and angular velocity C/d^2. If the pair instead have opposite strength, C and $-C$, they will move in unison through the fluid with a common velocity C/d, or conversely they will remain in place in an opposite ambient wind of strength $-C/d$. An isolated ring vortex, a smoke ring, of strength C interacts in this way with itself and propagates through the fluid with the speed C/d where d is the ring's diameter.

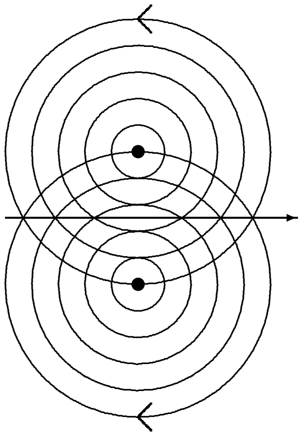

Two vortices with equal but opposite strength, C and $-C$, cause the cores of each other to move in the same direction with the same speed, here towards the right. The same picture is valid for a cross section through the center of a smoke ring.

It is perhaps somewhat counterintuitive that a smoke ring should move in the same direction as the flow inside the ring. A smoke ring is formed by blowing smoke-laden air at high speed through a circular opening made by the lips. The initial burst of air will carry the ring forward, but the ring may be observed to continue forwards way beyond the range of the initial burst.

In the wake of a moving cylinder a slower moving regular pattern of vortices, called the *von Kármán vortex street*, will be formed at Reynolds numbers below the onset of turbulence (see for example [39, ch. 5] or [15, p. 155]) for a more quantitative discussion of this phenomenon).

21.3 Viscous cylindrical vortices

We now return to the question of the behavior of vortices in the presence of viscosity by reconsidering the Rankine vortex (21-1). When two partial solutions don't match, it is sometimes possible to find a smooth interpolating function which coincides with the partial solutions in most of their respective domains. For the Rankine vortex we may take

$$v_\phi = \frac{\Omega c^2}{r}\left(1 - \exp\left(-\frac{r^2}{c^2}\right)\right) . \tag{21-8}$$

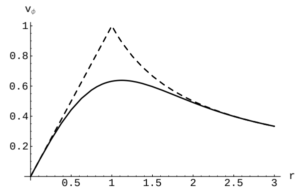

The fully drawn interpolating curve makes a smooth connection between the core and the outer flow (here with $c = \Omega = 1$).

This expression approaches the Rankine solution for both $r \ll c$ and for $r \gg c$, but the shear stress is now continuous everywhere and the problem with Newton's third law has disappeared. The central depression of the liquid surface is somewhat shallower than for the Rankine vortex,

$$L - h_0 = k\frac{\Omega^2 c^2}{g_0} , \qquad k = 0.693\ldots \tag{21-9}$$

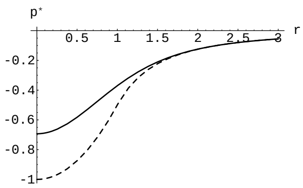

The effective pressure for the Rankine vortex (dashed) and the interpolating vortex (here with $c = \Omega = g_0 = 1$).

with a coefficient that has been determined by numeric integration.

Diffusive spin-down of a free vortex

The resolution of the stress problem comes at a price, because the interpolating vortex cannot be stable on its own in a viscous fluid. The shear stress will dissipate kinetic energy everywhere in the fluid and make the vortex spin down. The largest shear stress is found just outside the core and will primarily cause the core's rotation to slow down and expand its radius. The flow at greater distances from the core is left undisturbed, at least until the expanding core reaches it.

Assuming that the azimuthal velocity field retains its cylindrical form $v_\phi(r,t)$ at all times, the time-dependent Navier-Stokes equation for this field becomes

$$\boxed{\frac{\partial v_\phi}{\partial t} = \nu\frac{\partial}{\partial r}\left(\frac{1}{r}\frac{\partial(r v_\phi)}{\partial r}\right)} , \tag{21-10}$$

which is quite analogous to the momentum diffusion equation (17-7), except for the extra complication of cylindrical coordinates. Given an initial field $v_\phi(r,0)$, this equation will always yield a solution.

One may by insertion directly verify that the solution which for $t = 0$ equals the interpolating vortex (21-8) is the so-called *Oseen-Lamb vortex*,

$$v_\phi(r,t) = \frac{\Omega c^2}{r}\left(1 - \exp\left(-\frac{r^2}{c^2 + 4\nu t}\right)\right) . \tag{21-11}$$

The core radius, $c(t) = \sqrt{c^2 + 4\nu t}$, grows with time while the angular velocity $\Omega(t) = \Omega c^2/(c^2 + 4\nu t)$ and the central depression $L - h_0 = k\Omega^2 c^4/g_0(c^2 + 4\nu t)$ both decrease with time. The time scale for spin-down, $t_c = c^2/4\nu$, is recognized as the typical momentum diffusion time scale (see page 289). There are many other exact solutions to (21-10) (see problems 21.6 and 21.7).

Vortex sustained by secondary flow

Intuitively, it seems as if the natural tendency for the vortex core to expand could be counteracted by a sufficiently strong steady radial inflow, $v_r(r)$. Since the radial inflow of fluid cannot accumulate at the center of the vortex, there must necessarily also be a steady axial outflow, v_z. The relation between radial and axial flow is given by the equation of continuity, which in cylindrical coordinates takes the form (see problem 21.3)

$$\frac{1}{r}\frac{d(rv_r)}{dr} + \frac{\partial v_z}{\partial z} = 0 \ . \tag{21-12}$$

Solving for v_z we obtain,

$$\boxed{v_z(r,z) = w(r) - \frac{z}{r}\frac{d(rv_r(r))}{dr}} \ , \tag{21-13}$$

where $w(r)$ is an arbitrary function that specifies the axial flow at $z = 0$. The second term represents the accumulated radial inflow.

Including advective terms, the equation for the steady cylindrical azimuthal field becomes,

$$\boxed{\frac{v_r}{r}\frac{d(rv_\phi)}{dr} = \nu\frac{d}{dr}\left(\frac{1}{r}\frac{d(rv_\phi)}{dr}\right)} \ . \tag{21-14}$$

Given a radial inflow $v_r(r)$, this equation will always yield a solution. Conversely, we may use this equation to determine the radial inflow that is needed to maintain any choice of azimuthal flow, $v_\phi(r)$.

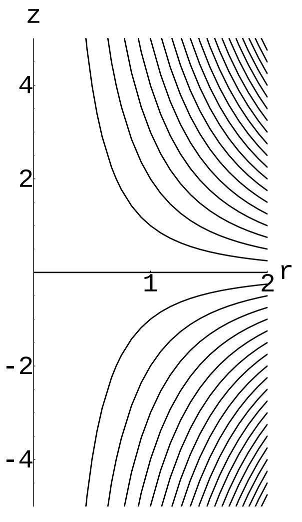

Streamlines for secondary flow in the Burgers vortex. The pattern is mirror symmetric in $z = 0$. The actual streamlines are spirals that circle around the center of the vortex while contracting and moving upwards or downwards along the axis.

The Burgers vortex

These arguments may be verified by inserting the interpolating vortex (21-8) into (21-14). The complete flow pattern maintaining this vortex is (for $w = 0$),

$$v_\phi = \frac{\Omega c^2}{r}\left(1 - \exp\left(-\frac{r^2}{c^2}\right)\right) \ , \tag{21-15a}$$

$$v_r = -\frac{2\nu}{c^2} r \ , \tag{21-15b}$$

$$v_z = \frac{4\nu}{c^2} z \ . \tag{21-15c}$$

It is called the *Burgers vortex* and is in fact an exact solution to the full set of steady-flow Navier-Stokes equations (see problem 21.3). The scale of the secondary flow is set by the inverse of the typical momentum diffusion time, $1/t_c = 4\nu/c^2$, but that is not particularly surprising, since the purpose of the secondary flow is to counteract core expansion. For $\nu \to 0$, the secondary flow disappears, as one would expect.

Angular momentum conservation

The basic mechanism that shapes a steady vortex in the presence of radial inflow, is conservation of angular momentum. The angular momentum of a fluid particle of mass dM is $d\mathcal{L}_z = rv_\phi\, dM$, and since the mass is always constant, it follows that the specific angular momentum, rv_ϕ, must be constant, and the vortex gets the characteristic shape, $v_\phi \approx C/r$. Formally, this may also be seen from (21-14). Provided that the radial inflow is so strong that the right hand side can be disregarded, we obtain $d(rv_\phi)/dr \approx 0$ from the left hand side, so that rv_ϕ must be constant. The precise shape of the radial inflow does not matter, neither for the intuitive nor the formal argument, as long as the inflow is strong enough.

Even if the inflow is strong enough for large r, it will never be strong enough for sufficiently small r. Since the flow along the axis $v_z(r, z)$ should be finite for $r \to 0$, it follows from the second term in (21-13) that $v_r \sim r$ close to the center of the vortex. Thus, there will always be a point near the axis where the radial inflow has become so small that the right hand side of (21-14) becomes comparable to the left hand side. This point defines the core boundary $r = c$, and deep inside the core the right hand side will dominate, so that the azimuthal field becomes that of a solidly rotating body, $v_\phi = \Omega r$. For sufficiently strong asymptotic inflow, any flow-sustained steady vortex will thus in its gross structure resemble a Rankine vortex with core radius $c \approx \sqrt{C/\Omega}$.

Steady vortex with localized axial jet

The Burgers vortex does not resemble a bathtub vortex much, because v_z is independent of r, whereas in a real bathtub the axial flow is supposed to converge upon the drain-hole. In naturally born vortices, the axial outflow is mostly confined to take place inside a certain drain radius, a kind of *axial jet*. We postpone the discussion of vortices with an open liquid surface, more akin to what is seen in a real bathtub, to section 21.4.

Assuming that $v_z = 0$ outside a certain drain radius $r \gtrsim a$, it follows from the explicit expression for the axial flow (21-13), that we must have both $w(r) = 0$ and $d(rv_r)/dr = 0$ in this region. Consequently, the radial flow must be of the form,

$$v_r = -\frac{q}{r} , \qquad (r \gtrsim a) , \tag{21-16}$$

where q is a positive constant, that sets the scale of the radial inflow. The total volume of fluid that enters the vortex over an axial length L is $Q = -2\pi r L v_r = 2\pi q L$. Mass conservation tells us that this must equal the amount of fluid that is carried away from the central region by the axial jet.

Using this form of the radial flow, it may be verified by insertion that the most general solution to (21-14) may be written,

$$rv_\phi = C + Ar^{2-q/\nu} , \qquad (r \gtrsim a) \tag{21-17}$$

where C and A are constants. The second term decays at infinity only if $q > 2\nu$, and this confirms that the radial inflow must have a certain strength for the azimuthal flow to approach, $v_\phi \approx C/r$, at large distances.

Advective spin-up of a vortex

To see how a vortex with a localized axial jet is "cranked up" by a steady radial inflow, we assume that $q \gg 2\nu$ such that we may disregard viscosity outside the drain. The time-dependent azimuthal equation is in this region dominated by the advective terms and becomes,

$$\boxed{\frac{\partial v_\phi}{\partial t} + \frac{v_r}{r}\frac{\partial (r v_\phi)}{\partial r} = 0} . \tag{21-18}$$

Inserting the radial field (21-16), it takes the form

$$\frac{\partial (r v_\phi)}{\partial t} = 2q \frac{\partial (r v_\phi)}{\partial \xi} ,$$

where $\xi = r^2$. The most general solution to this equation is an arbitrary function of $\xi + 2qt$, which we shall write as

$$v_\phi(r,t) = \frac{f\left(\sqrt{r^2 + 2qt}\right)}{r} , \qquad (r \gtrsim a) \tag{21-19}$$

where $f(r) = r v_\phi(r, 0)$ is the initial specific angular momentum.

At any sufficiently late time $t \gg a^2/2q$, the numerator will be approximatively independent of r for all $a \lesssim r \ll \sqrt{2qt}$. The typical vortex tail, $v_\phi \approx C/r$ thus spreads out from the drained region of the vortex with a time-dependent circulation "constant" $C \approx f(\sqrt{2qt})$. As time goes by, the spreading vortex probes the initial velocity profile to farther and farther distances. Although the circulation "constant" changes at a slower and slower rate because of the squareroot, a steady vortex is never reached unless the initial specific angular momentum distribution $f(r)$ itself approaches a constant for $r \to \infty$.

These arguments show that it is in fact not so easy to spin up a steady vortex by means of radial inflow in a non-rotating system, for the simple reason that it requires infinite angular momentum to be present in the flow to begin with. In the laboratory, a steady vortex can instead be created by rotating the container at a steady rate thus providing the system with an everlasting source of angular momentum (see section 25.6).

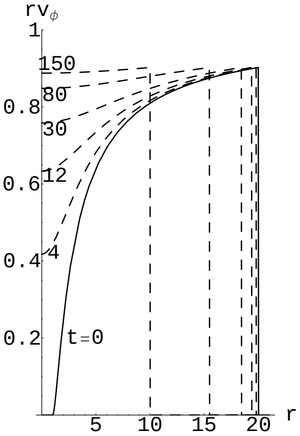

"Movie" of advective spin-up of a vortex from an initial bump in the specific angular momentum (fully drawn curve). The advection parameter is $q = 1$ and the bump lies in the interval $1 \le r \le 20$. The angular momentum distribution is progressively flattened in the course of time (dashed curves), while being drawn closer to the drain. It disappears completely into the drain for $t = 200$.

Discuss picture better

The process of getting out of a real bathtub cannot avoid leaving a certain amount of angular momentum in the water. It is this angular momentum that the inflow picks up and sends down the drain while the bathtub is being emptied (see problem 21.10). A real bathtub vortex may change speed and even stop up and reverse its sense of rotation depending on the details of how you got out of the water. In a bathtub of ordinary size the accidental initial angular momentum distribution is normally much larger than what can be provided by the slowly rotating Earth.

* 21.4 Bathtub-like vortices

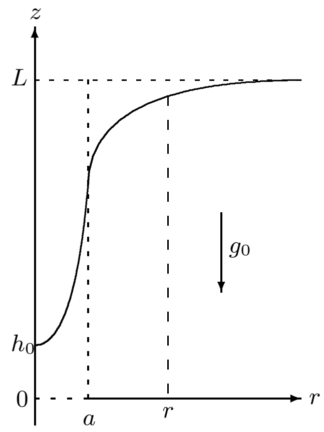

Bathtub-like liquid vortex with open surface. At $z = 0$ there is a drain-hole of radius a, and the "tub" has essentially infinite extension in the radial direction. There is a central depression of height h_0 and the asymptotic liquid level is $z = L$. Mass conservation guarantees that the volume of fluid flowing in through the cylinder of radius r equals the volume flowing out through the drain surface $z = 0$ inside r.

Consider a steady liquid vortex with a rotationally invariant surface, $z = h(r)$. The vortex is held in a non-rotating vertical container that is drained through a circular hole of radius $r = a$ situated at the bottom at $z = 0$. The container radius $r = b$ is assumed to be essentially infinite in comparison with the drain radius. The complications that arise in a rotating container are discussed in the following section[1].

Effects of an open liquid surface

The existence of an open liquid surface influences the vortex in two ways. Mass conservation creates a coupling between surface height and the radial flow, and the constancy of the surface pressure creates (in the nearly ideal case) a coupling between the height and the azimuthal flow.

The streamlines at the fluid surface must be tangential to the surface, $v_z(r, h(r)) = h'(r)v_r(r)$, and combining this with the expression for the axial flow (21-13), we obtain the exact relationship,

$$\boxed{\frac{1}{r}\frac{d(rv_r h)}{dr} = w} \quad . \tag{21-20}$$

In nearly ideal flow, the stress vector is dominated by the (true) pressure, which we normalize so that the constant surface value is zero. Writing $p^* = \rho_0 g_0 h$ and using $p^* = p + \rho_0 g_0 z$, we obtain

$$p(r, z) = \rho_0 g_0 (h(r) - z) \ . \tag{21-21}$$

Evidently, it vanishes at the surface as it should. The effective pressure must in the same approximation also provide the necessary centripetal force for the circulating motion, $dp^*/dr = \rho_0 v_\phi^2/r$, so that we get

$$\boxed{\frac{dh}{dr} = \frac{v_\phi^2}{g_0 r}} \quad . \tag{21-22}$$

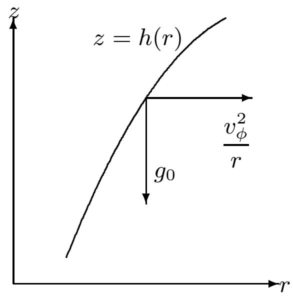

A fluid particle sitting on the rotating surface of the vortex is subject to gravity and centrifugal force. The projections of these forces on the surface cancel in the leading approximation.

If one writes this equation as $-g_0 h' + v_\phi^2/r = 0$, it expresses that at the surface the tangential component of gravity balances the tangential component of the centrifugal force. A fluid particle at the surface experiences no tangential force in this approximation.

Given the drain-flow $w(r)$, the three coupled ordinary differential equations (21-14), (21-20), and (21-22) determine the unknown functions, v_ϕ, v_r and h. They can in general only be solved by numerical integration.

[1]This section is in part inspired by T. S. Lundgren, *The vortical flow above the drain-hole in a rotating vessel*, J. Fluid Mech. **155**, 381 (1985).

Choice of drain-flow

A convenient choice of w is pure "plug-flow" with a constant downwards velocity W inside the drain,

$$w(r) = \begin{cases} -W & (r < a) \\ 0 & (r > a) \end{cases} . \tag{21-23}$$

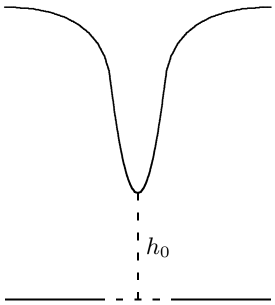

Torricelli's law applied to the central streamline leads to $W = \sqrt{2g_0h_0}$ for a gravity-driven vortex.

One may imagine that this flow is controlled by a suction device removing liquid through the drain at a constant volume rate $Q = \pi a^2 W$. Alternatively, if gravity is the draining force, the velocity may in the nearly ideal case be estimated from Torricelli's law (15-19),

$$W \approx \sqrt{2g_0h_0} , \tag{21-24}$$

which is the free-fall velocity from the center of the surface depression.

From (21-20) we obtain the corresponding radial inflow,

$$v_r(r) = -\frac{Wa}{2h(r)} \begin{cases} \dfrac{r}{a} & (r < a) \\ \dfrac{a}{r} & (r > a) \end{cases} . \tag{21-25}$$

Since for $r \to \infty$ we have $h(r) \to L$, the asymptotic inflow parameter is $q = Wa^2/2L$. The cusp at $r = a$ creates an unphysical jump in stress at the edge of the drain, as we saw for the Rankine vortex. It is also here possible to choose a softer form than (21-23) leading to a radial flow which interpolates smoothly between the two regions (see problem 21.14).

Radial and axial Reynolds numbers

The most important number is the ratio between advective and viscous terms in the azimuthal equation, which at great distances becomes

$$\mathsf{Re}_r = \frac{r\,|v_r|}{\nu} \approx \frac{q}{\nu} = \frac{Wa^2}{2L\nu} . \tag{21-26}$$

Comparing with (21-17) we conclude that the asymptotic form of the azimuthal field will only be filament-like, $v_\phi = C/r$, for $\mathsf{Re}_r > 2$. Another Reynolds number is obtained from the Poiseuille-like flow through the drain

$$\mathsf{Re}_z = \frac{2aW}{\nu} = \frac{4L}{a}\mathsf{Re}_r . \tag{21-27}$$

Normally $L \gg a$, so that Re_z is much larger than Re_r.

Example 21.4.1: A bathtub is filled with water to a height $L = 50$ cm. When the plug (of radius $a = 3$ cm) is pulled from the drain, the water falls freely through the drain with a velocity that maximally can be $W \approx \sqrt{2g_0L} \approx 3.1$ m s^{-1}, leading to $\mathsf{Re}_r \approx 4000$ and $\mathsf{Re}_z \approx 2.6 \times 10^5$. These numbers are so large that we are probably not justified in using the present laminar theory.

Estimate of the depth of the depression

Were it not for the variation in surface height $h(r)$, the radial flow inside the drain would be linear in r, and the inner solution would be identical to the Burgers vortex (21-15). The central depression of the surface quickens the radial inflow close to the center and makes the core radius smaller than for the Burgers vortex. Estimating the core radius of the bathtub vortex by the same condition as for the Burgers vortex, *i.e.* $rv_r \approx -2\nu$, we find

$$c \approx 2\sqrt{\frac{\nu h_c}{W}} \ , \tag{21-28}$$

where $h_c = h(c)$ is the surface height at the core boundary. This quantity may also be determined by integration of (21-22),

$$L - h_c = \int_c^\infty \frac{v_\phi^2}{g_0 r}\, dr \approx \frac{C^2}{2g_0 c^2} \approx \frac{C^2 W}{8\nu g_0 h_c} \ , \tag{21-29}$$

where we have estimated the integral by taking $v_\phi \approx C/r$. It is a quadratic equation that may be solved for h_c, but it is better to estimate $h_c \approx (L + h_0)/2$ and obtain a closed expression for the height of the central depression

$$h_0 \approx \sqrt{L^2 - \frac{C^2 W}{2g_0 \nu}} \ . \tag{21-30}$$

If the argument of the squareroot becomes negative, the central dip in the surface plunges right through the drain, thereby violating the basic assumptions behind the model. It is convenient to introduce the dimensionless quantity

$$\gamma = \frac{C^2 W}{2g_0 \nu L^2} \ , \tag{21-31}$$

such that $h_0 = L\sqrt{1-\gamma^2}$. The condition $\gamma \leq 1$ is not rigorous because it is found from an estimate, but it must be expected that there is an upper limit to this quantity in the neighborhood of unity.

Numeric integration

The numeric integration of the coupled differential equations is sufficiently tricky to warrant a closer look. The equations are first reexpressed in terms of dimensionless variables and functions

$$\xi = \frac{r^2}{a^2} \ , \tag{21-32a}$$

$$w(r) = -Wf(\xi) \ , \tag{21-32b}$$

$$h(r) = Lg(\xi) \ , \tag{21-32c}$$

$$rv_\phi(r) = Cu(\xi) \ , \tag{21-32d}$$

$$rv_r(r)h(r) = -\frac{1}{2}Wa^2 v(\xi) \ . \tag{21-32e}$$

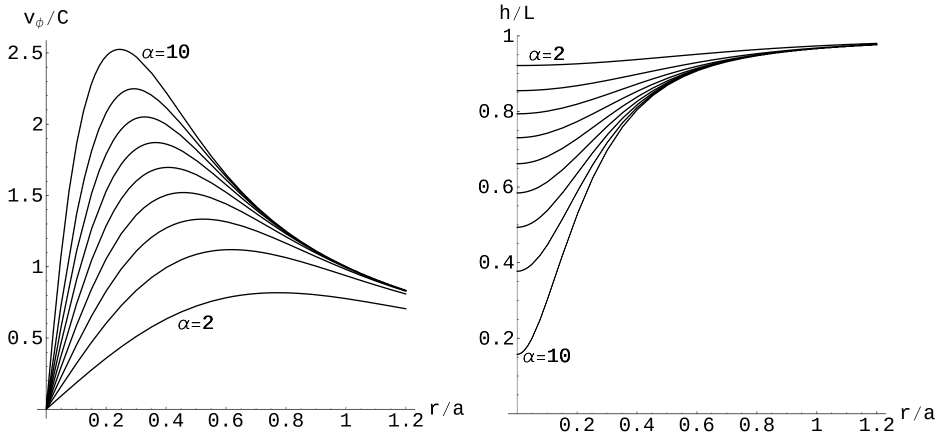

Figure 21.1: *Azimuthal flow (left) and surface depression (right) for* $\beta = 0.18284$ *and* $\alpha = 2, 3, \ldots, 10$. *The core radius corresponds roughly to the top in* v_ϕ *and shrinks with growing secondary flow* (α) *whereas the depression deepens.*

The coupled equations now take the form

$$v' = f \tag{21-33a}$$

$$u'' = -\alpha \frac{u'v}{\xi g} \tag{21-33b}$$

$$g' = \beta^2 \frac{u^2}{\xi^2} \tag{21-33c}$$

where a prime denotes the derivative after ξ. The dimensionless functions, u, v, and g are all required to approach unity for $\xi \to \infty$. The dimensionless drain-function f is for plug-flow a simple step function,

$$f(\xi) = \begin{cases} 1 & (\xi < 1) \\ 0 & (\xi > 1) \end{cases} . \tag{21-34}$$

but may in principle be freely chosen.

The constants

$$\alpha = \frac{q}{2\nu} = \frac{Wa^2}{4L\nu} , \qquad \beta = \frac{C}{a\sqrt{2g_0 L}} , \tag{21-35}$$

should be viewed as dimensionless measures of the strength of the asymptotic radial inflow $rv_r \approx -q = -Wa^2/2L$ and the asymptotic circulation $rv_\phi \approx C$. Since $\gamma = 4\alpha\beta^2$, the constants must satisfy

$$1 < \alpha \lesssim \frac{1}{4\beta^2} . \tag{21-36}$$

For $\alpha < 1$ the asymptotic azimuthal flow (21-17) will not approach C/r asymptotically, and for $\alpha \gtrsim 1/4\beta^2$ the depression (21-30) will plunge through the drain-hole. The last inequality is based on rather coarse estimates and should not be expected to be exactly fulfilled.

The coupled equations are best solved by imposing boundary conditions at $\xi = 0$ where $u(0) = 0$, $u'(0) = s$, $v(0) = 0$, and $g(0) = k$. Starting with some choice of s and k a search is made for those values that lead to fulfillment of the boundary conditions at infinity, $u(\infty) = v(\infty) = g(\infty) = 1$. The result is shown in fig. 21.1 for the particular value $\beta = 0.18284$, which allows for a maximal value of $\alpha = 10$. Numerically, the critical limit to non-plunging behavior is determined by the appearance of numerical instabilities. The limit is found to be very close to $\gamma = 4\alpha\beta^2 \approx 1.345$ for nearly all values of $\alpha \gtrsim 2$.

Problems

21.1 Calculate the kinetic energy of the Rankine vortex inside a radial distance $r \leq R$ and axial length L .

21.2 Show that the circulation around a Rankine vortex is independent of the curve, as long as it encircles the axis of the vortex and lies entirely outside the core.

21.3 Assume that the velocity fields $v_{r,\phi,z}$ in cylindrical coordinates only depend on r and z. Show that the Navier-Stokes equations become

$$\frac{\partial v_\phi}{\partial t} + v_r \frac{\partial v_\phi}{\partial r} + \frac{v_r v_\phi}{r} + v_z \frac{\partial v_\phi}{\partial z} = \nu \left(\frac{\partial^2 v_\phi}{\partial r^2} + \frac{1}{r}\frac{\partial v_\phi}{\partial r} - \frac{v_\phi}{r^2} + \frac{\partial^2 v_\phi}{\partial z^2} \right) , \tag{21-37a}$$

$$\frac{\partial v_r}{\partial t} + v_r \frac{\partial v_r}{\partial r} - \frac{v_\phi^2}{r} + v_z \frac{\partial v_r}{\partial z} = \nu \left(\frac{\partial^2 v_r}{\partial r^2} + \frac{1}{r}\frac{\partial v_r}{\partial r} - \frac{v_r}{r^2} + \frac{\partial^2 v_r}{\partial z^2} \right) - \frac{1}{\rho_0}\frac{\partial p^*}{\partial r} , \tag{21-37b}$$

$$\frac{\partial v_z}{\partial t} + v_r \frac{\partial v_z}{\partial r} + v_z \frac{\partial v_z}{\partial z} = \nu \left(\frac{\partial^2 v_z}{\partial r^2} + \frac{1}{r}\frac{\partial v_z}{\partial r} + \frac{\partial^2 v_z}{\partial z^2} \right) - \frac{1}{\rho_0}\frac{\partial p^*}{\partial z} , \tag{21-37c}$$

with the incompressibility condition

$$\frac{\partial v_r}{\partial r} + \frac{v_r}{r} + \frac{\partial v_z}{\partial z} = 0 \tag{21-38}$$

21.4 Calculate the streamlines for the Burgers vortex.

21.5 Calculate the exact pressure for the Burgers vortex.

21.6 a) Show that the so-called Taylor vortex

$$\boxed{v_\phi(r,t) = \tau \frac{r}{t^2} e^{-r^2/4\nu t}} , \tag{21-39}$$

is a solution to (21-10) where τ is a constant with dimension of time. b) Calculate the total angular momentum for a stretch of length L of the Taylor vortex and show that it is constant in time.

21.7 Assume that a free cylindrical vortex only depends on the dimensionless variable

$$\xi = \frac{r^2}{4\nu t} . \tag{21-40}$$

and assume that

$$v_\phi(r,t) = \frac{F(t)}{r} f(\xi) , \tag{21-41}$$

where $F(t)$ is a time-dependent factor.

a) Find a differential equation for $f(\xi)$.

b) Show that $F(t) \sim t^{-\alpha}$ where α is a dimensionless parameter.

c) Show that the solution is

$$f_\alpha(\xi) = \sum_{n=0}^{\infty} \frac{(n+\alpha)!}{n!\,\alpha!}(-1)^n \frac{\xi^{n+1}}{(n+1)!} \tag{21-42}$$

d) Find a closed form for $\alpha = 0, 1, 2$ and draw the vortex shapes.

21.8 Show explicitly that the interpolating field (21-8) together with the Burgers secondary flow (21-15) is a solution to the Navier-Stokes equations for steady incompressible fluid, (18-1) and (18-2).

21.9 Assume that a vortex at $t = 0$ has the shape of an interpolating vortex (21-8) with radius b, and that there is a radial inflow identical to that of the Burgers vortex (21-15) corresponding to a radius a. Determine how the azimuthal flow of the original vortex converges upon the interpolating function of radius a.

21.10 The water in a bathtub originally rotates like a solid body, $v_\phi = \Omega r$, far from the drain. Determine the far field at a later time and the rate at which angular momentum flows in towards the drain.

21.11 Show that the equations for the tornado-like flow are solved by the following integrals

$$rv_r(r) = \frac{1}{L}\int_0^r r' w(r')\, dr' \tag{21-43}$$

$$f(r) = \frac{1}{\nu}\int_0^r v_r(r')\, dr' \tag{21-44}$$

$$rv_\phi(r) = 2\Omega \int_0^r r' e^{f(r')}\, dr' \tag{21-45}$$

where Ω is the angular velocity of the core.

21.12 a) Show that the divergence condition can be solved by means of a field $\psi(r, z)$ (a stream function) satisfying

$$\frac{\partial \psi}{\partial z} = rv_r\ , \qquad \frac{\partial \psi}{\partial r} = -rv_z \tag{21-46}$$

b) Show that the streamlines satisfy

$$\psi(r, z) = \text{const} \tag{21-47}$$

c) Show that the stream function for a cylindrically invariant vortex is

$$\psi(r, z) = rv_r(r)z - \int rw(r)dr \tag{21-48}$$

and use this result to find the streamlines for the various cylindrically invariant vortices.

21.13 Consider a tornado-like vortex with $h(r) = L$. Show that the vortex theory of section 21.4 leads to a solution

$$v_\phi = \begin{cases} \dfrac{\Omega c^2}{r}\left(1 - e^{-r^2/c^2}\right) , & (r < a) \\[2ex] \dfrac{\Omega c^2}{r}\left(1 + \frac{e^{-\alpha}}{\alpha - 1}\left(1 - \alpha\left(\frac{a^2}{r^2}\right)^{\alpha - 1}\right)\right) , & (r > a) \end{cases} . \tag{21-49}$$

where Ω is the angular velocity of the core and

$$c = \frac{a}{\sqrt{\alpha}} . \tag{21-50}$$

is the core radius.

21.14 Assume that the drain-flow is "soft"

$$w(r) = -We^{-r^2/a^2} , \tag{21-51}$$

and determine the radial flow.

